ACS OMEGA

http://pubs.acs.org/journal/acsodf

Article

Mapping Peptide–Protein Interactions by Amine-Reactive Cleavable Photoaffinity Reagents

Dimitris Korovesis,[&] Vanessa P. Gaspar,[&] Hester A. Beard,[&] Suyuan Chen, René P. Zahédi,* and Steven H. L. Verhelst*

Cite This: *ACS Omega* 2023, 8, 25487–25495

Read Online

ACCESS | Metrics & More | Article Recommendations | Supporting Information

ABSTRACT: Photoaffinity labeling followed by tandem mass spectrometry is an often used strategy to identify protein targets of small-molecule drugs or drug candidates, which, under ideal conditions, enables the identification of the actual drug binding site. In the case of bioactive peptides, however, identifying the distinct binding site is hampered because of complex fragmentation patterns during tandem mass spectrometry. We here report the development and use of small cleavable photoaffinity reagents that allow functionalization of bioactive peptides for light-induced covalent binding to their protein targets. Upon cleavage of the covalently linked peptide drug, a chemical remnant of a defined mass remains on the bound amino acid, which is then used to unambiguously identify the drug binding site. Applying our approach to known peptide–drug/protein pairs with reported crystal structures, such as the calmodulin–melittin interaction, we were able to validate the identified binding sites based on structural models. Overall, our cleavable photoaffinity labeling strategy represents a powerful tool to enable the identification of protein targets and specific binding sites of a wide variety of bioactive peptides in the future.

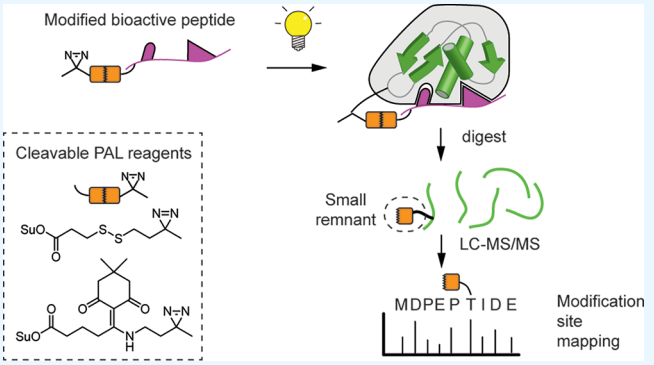

INTRODUCTION

Interactions between proteins and peptides play a crucial role in various physiological and pathophysiological processes. Bioactive peptides are either endogenously produced or are exogenous and enter the human body through other organisms or ingestion of food and drugs. Examples include peptide hormones, such as angiotensin and glucagon, snake venom peptides,[1] and food-derived peptides.[2] Detailed knowledge of the interaction of such bioactive peptides with their protein receptors may lead to the design of analogs with increased potency and may thus form a basis for the development of new therapeutic agents. For instance, the human glucagon-like peptide-1 (GLP-1) analog semaglutide has been designed to provide improved pharmacokinetics and has been approved by the FDA for the treatment of type 2 diabetes.[3]

Many polypeptide ligands in the body are generated by limited proteolysis of larger proproteins, such as cationic host defense peptides[4] (CHDP). However, in the past decade, it was discovered that the genome also includes small open reading frames (smORFs) that encode for polypeptides.[5] The amount of bioactive peptides in the human body is therefore many times larger than originally thought. Such peptides may also be utilized as a starting point for drug development. Consequentially, there is a need for the development of methods to map interactions between proteins and biologically active peptides, including peptide drug candidates.

Various methodologies have emerged to identify targets of drug-like molecules and bioactive peptides based on the increased stability of a protein upon a binding event. These include assays exploiting the lower susceptibility toward proteolysis[6,7] or thermal denaturation.[8] While these methods do not directly detect the actual binding event, chemical crosslinking combined with mass spectrometry (XL-MS) allows a more direct detection of the binding event and has been used particularly for the analysis of protein conformations and protein–protein interactions.[9−12] XL-MS reagents generally contain two lysine- or cysteine-reactive electrophiles, and more recently also combinations thereof, as well as combinations with photoreactive groups. These reagents covalently link two different protein molecules to form a "crosslinked peptide" upon proteolytic digestion. Crosslinked peptides are notoriously difficult to identify by MS^2, in part due

Received: May 4, 2023
Accepted: June 21, 2023
Published: July 7, 2023

https://doi.org/10.1021/acsomega.3c03064
ACS Omega 2023, 8, 25487–25495

to their higher mass and elevated charge states but particularly due to simultaneous fragmentation of both peptide chains leading to highly complex hybrid MS/MS spectra. Specific computational solutions have been developed to deal with the vast search space arising from the numerous possible combinations of peptide sequences, while MS-cleavable crosslinkers have been developed as a simple yet elegant alternative solution to this problem.[9,10,13] Through cleavage prior to MS detection, the individual peptides that form the crosslinked peptide can be analyzed and identified individually.[14] Both strategies, computational and cleavable linkers, have proven very powerful to study the structure of protein complexes[15] as well as organelle-wide protein/protein interactions.[16−18]

In contrast to conventional protein crosslinking studies, the elucidation of protein targets of small-molecule inhibitors or drugs usually only requires the identification of peptides derived from the target proteins, which is often accomplished through the use of photoaffinity labeling followed by MS.[19−22] Thus, in some cases, the modified amino acid residue can even be mapped, depending on the size as well as ionization and fragmentation behavior of the photoaffinity probe. In the case of peptide drugs, however, the identification of the protein/peptide binding sites suffers from the fragmentation of the bioactive peptide leading to hybrid MS/MS spectra similar to protein/protein crosslinks. To address these problems and improve the mapping of peptide−protein interactions, the use of cleavable photoreactive groups has recently started to be implemented.[23]

Here, we explore the identification of interactions between bioactive peptides and protein targets by modification of the peptide with different cleavable photoreactive groups. Whereas the photoaffinity labeling ensures covalent modification of the protein target, the cleavable linker ultimately results in a low-molecular-weight remnant on the amino acid residue of the target protein that had previously been covalently bound and represents the binding site. After proteolytic digestion and cleavage of the linker, this small remnant can be more easily detected by tandem MS than a crosslinked peptide ligand (Figure 1). Thus, we developed several cleavable photoreactive groups and evaluated their use for MS-based mapping of peptide binding sites on proteins. We show that interaction sites on different pairs of commercially available proteins and bioactive peptides can be unambiguously mapped using this strategy.

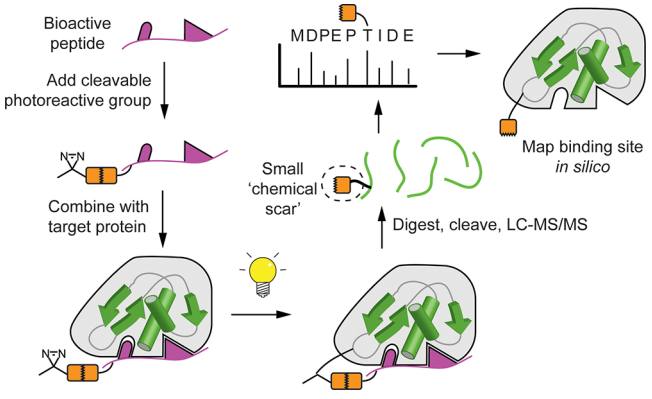

Figure 1. Overview of the here applied cleavable photoaffinity labeling (PAL) approach. A bioactive peptide is equipped with a cleavable diazirine building block and reacted with its target protein under the influence of light. Proteolytic digestion and cleavage will result in a remnant on the modified amino acid residue as remnant of the covalent binding of the bioactive peptide. MS^2 is then used to detect the modified residues, which are mapped in silico on the target protein to determine the area of interaction.

RESULTS AND DISCUSSION

Selection of Cleavable Linkers. We reasoned that cleaving off a "large" peptide drug from the side chain of a tryptic peptide would be beneficial for the identification of the binding site by tandem MS: it will mark the original binding site with a small remnant, and consequently, the size as well as the fragmentation of this modification is minimized. However, different linkers have varying cleavage efficiencies. Additionally, the remnants of the cleaved linker may have a pronounced effect on chromatographic behavior, ionization, and fragmentation of the tryptic peptide, as well as on database searches and identification. In order to select linkers that are easy to handle and efficient without compromising MS sensitivity and identification, we synthesized by solid-phase peptide synthesis (SPPS) two model tryptic peptides, LFLKSGVR and VKAALELAEQR (**1** and **2**), derived from *Escherichia coli* rpsD. These have (i) one Lys side chain modified by different MS-cleavable or chemically cleavable linkers (Scheme 1) and (ii) were previously identified by us to have a strong difference in LC−MS signals, therefore representing a "poor flyer" (LFLKSGVR) and a "good flyer" peptide (VKAALELAEQR), respectively.[24] The linkers connect the tryptic peptide to an aryl group as a model for a bioactive small-molecule or peptide. As controls, unmodified (a) or acetyl-modified (b) peptides were included. As linkers, we incorporated the following: (c) a sulfoxide linker (SF),[25] (d) an asymmetric and (e) symmetric urea linker (UA and UB),[26] which are all MS-cleavable using collision-induced dissociation (CID), (f) an azobenzene (AZ), which can be reductively cleaved,[27,28] (g) a disulfide (DS), which can be reductively cleaved or during MS by electron transfer dissociation,[29] and (f) a 2-acyl-dimedone-based linker (DDE), which cleaves under treatment with a low percentage of hydrazine.[30,31]

We analyzed all peptide standards by LC−MS/MS to determine chromatographic behavior and fragmentation in MS^2. The chemically cleavable AZ, DDE, and DS linker versions of the model peptides **1** and **2** were analyzed with and without prior cleavage of the linker by 25 mM $Na_2S_2O_4$, 2% hydrazine, or 0.5 M DTT, respectively.

While the nonmodified peptides as well as the DDE-cleaved peptides (dde; for all abbreviated linkers, small letters indicate cleaved forms) could be identified confidently with all fragmentation modes, DDE, ds, AZ, SF, and sf peptides performed overall better with CID and HCD than with ETD and EtHCD (Tables S1 and S2). The az peptides performed poorly with all fragmentation modes. We, therefore, focused our attention on DDE and DS and tested the efficiency of cleavage with 2% hydrazine and 0.5 M DTT, respectively, yielding cleavage rates of >95 and >98% (Figure 2C). For both linkers, the cleaved peptides (dde and ds) showed similar intensities to their unmodified controls. Notably, the retention times of the dde peptides were almost identical to those of the corresponding nonmodified peptides (Figure 2A,C and Tables S1 and S2), such that retention times can be used to add another level of confidence to dde−peptide identifications. Overall, the assessment suggested that the chemically cleavable

https://doi.org/10.1021/acsomega.3c03064
ACS Omega 2023, 8, 25487−25495

Scheme 1. Synthesis of Model Tryptic Peptides Incorporating Different Cleavable Linkers[a]

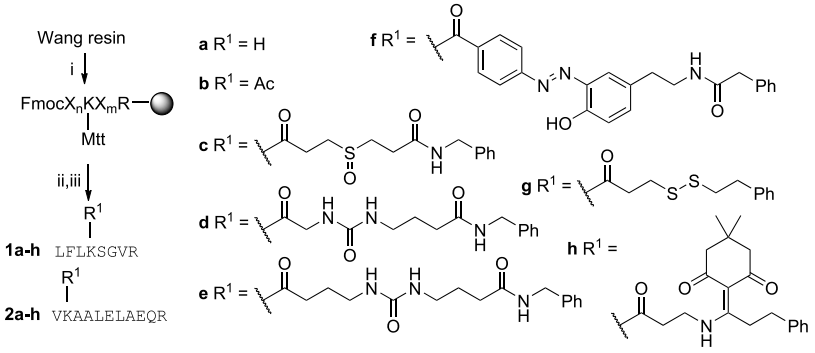

[a]X_n and X_m stand for the multiple amino acid residues flanking the modified lysine. Reagents and conditions: (i) elongation by repeated treatment with 20% piperidine/DMF, then Fmoc-aa-OH, DIC, HOBt, DMF; (ii) 1% TFA/DCM, then coupling of the individual linkers (see Supporting Information Schemes S1−S5 for details); (iii) TFA/TIS/H_2O 95/2.5/2.5.

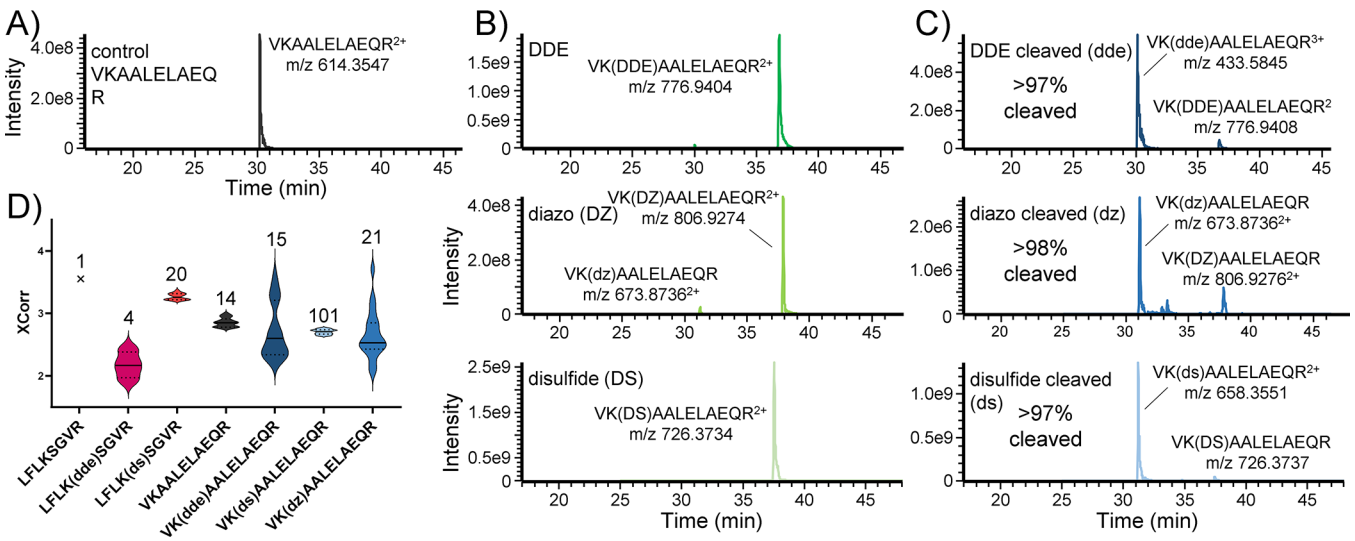

Figure 2. Different linker chemistries and their behavior during LC−MS/MS. (A) Extracted ion chromatogram (XIC) of the tryptic peptide VKAALELAEQR. (B,C) XICs of the intact (DDE, DZ, and DS) and cleaved (dde, dz, and ds) linker-labeled variants of VKAALELAEQR. Approximately 200 fmol of total peptides was loaded on-column; shown are the dominating charge states. (D) Sequest HT XCorr distribution and number of high-confidence peptide-spectrum matches for the cleaved DDE (dde), diazo (dz), and disulfide (ds) linker-labeled peptides LFLKSGVR and VKAALELAEQR after the respective treatment, 2 fmol of total peptides loaded on-column, no dynamic exclusion used. LFLKSGVR could not be identified with the cleaved diazo linker.

disulfide and DDE linkers were most desirable for the development of the cleavable photoaffinity reagents.

Design and Synthesis of Cleavable Photoaffinity Labels. We next set out to design and synthesize reagents to equip bioactive peptides with a cleavable photoaffinity group. As a photoreactive group, we chose an aliphatic diazirine. Upon UV irradiation, it generates a carbene species that inserts in nearby CH and heteroatom-H bonds, enabling crosslinking to many different amino acid side chains. Recent studies also revealed that UV irradiation can isomerize diazirines to diazo species, which display a preference toward labeling of carboxylic acids (Asp, Glu, and the free C-terminus).[32] More importantly, the aliphatic diazirine is the smallest known photoreactive group, less likely to result in a steric clash with the target protein than bulkier photoreactive groups, such as benzophenone. In addition, diazirines result in lower nonspecific PAL.[33] The diazirine building blocks were synthesized with a thiol or amine function, as outlined in Scheme 2A. Building blocks **6** and **8** were coupled to mercaptopropionic acid or DDE derivative **12**, respectively, and subsequently esterified with *N*-hydroxysuccinimide (NHS). This provided fully functionalized cleavable photoaffinity labels **9** and **13** with an NHS-activated ester, which allows facile coupling to the N-terminus or lysine side chain of a peptide (Scheme 2B).

Peptide Modification and Photoaffinity Labeling. At this point, we tested incorporation of the cleavable photoaffinity building blocks **9** and **13** into bioactive peptides. Importantly, our building blocks can not only be used during the full chemical synthesis of bioactive peptides on a solid support but can also be attached to commercially available peptides without the need for a peptide synthesizer. We here selected several commercially available bioactive peptides with a known protein receptor that was also commercially available in a purified form and whose crystal structure had been reported in the RCSB Protein Data Bank.[34] These included glucagon, which is a peptide hormone that binds and activates the GLP-1 receptor (GLP-1R), and melittin, which is a component of honeybee venom and inhibits the action of calmodulin. After modification of the bioactive peptides, we

https://doi.org/10.1021/acsomega.3c03064
ACS Omega 2023, 8, 25487−25495

Scheme 2. Synthesis of Amino Reactive Cleavable Photoaffinity Labels: (A) Synthesis of Building Blocks 9 and 13 and (B) Glucagon and Melittin That Were Reacted with Building Blocks 9 or 13 in the Presence of DIPEA in DMSO and Obtained as Predominantly Monosubstituted Photoaffinity Peptides[a]

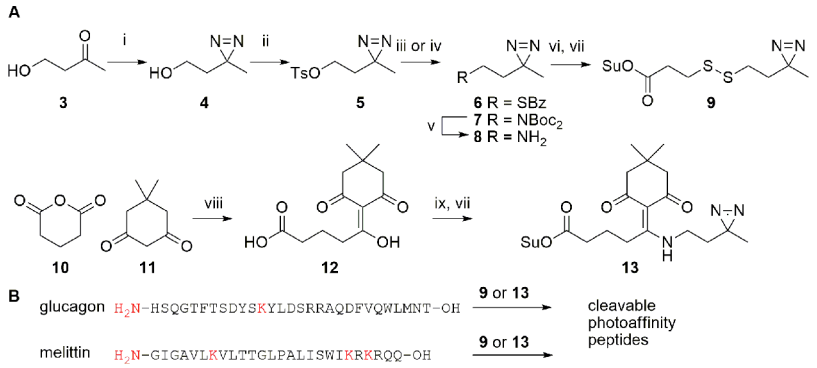

[a]Reagents and conditions: (i) 1. NH_3/MeOH, then NH_2OSO_3H; 2. I_2, Et_3N. (ii) TsCl, pyridine, 0 °C and then at RT. (iii) Thiobenzoic acid, Et_3N, MeCN, reflux. (iv) Boc_2NH, K_2CO_3, DMF, 80 °C. (v) TFA/DCM. (vi) 1. Dipyridyl-disulfide, pyrrolidine, MeOH/THF; 2. Mercaptopropionic acid, Et_3N, DMF. (vii) *N*-Hydroxysuccinimide, DIC, DCM. (viii) DMAP, DCM, 0 °C and then at RT. (ix) Compound **8**, Et_3N, EtOH, reflux.

evaluated the photoaffinity labeling by a gel-shift assay (Figure 3A,B). We focused on peptides modified by building block **13** because the disulfide cleavable linker in building block **9** is cleaved in reducing gels. After incubation with the target protein and irradiation with UV light, proteins were separated by SDS-PAGE followed by silver staining for visualization. For the GLP-1R, a clear gel shift was observed upon incubation with building block **13**-modified glucagon (Figure 3A), whereas for calmodulin, a slight shift was visible that appeared as a smear above the band (Figure 3B).

Next, we excised the gel bands and processed them for LC−MS/MS analysis. In short, gel bands were washed, and proteins were in-gel reduced (this step was skipped for the DS linker samples and the DMSO-treated control samples), alkylated, and in-gel digested with subtilisin.[35] As a broad-specificity protease, subtilisin can yield a substantially higher sequence coverage than trypsin when mapping modification sites on purified protein samples.[36] Extracted peptides were treated with a hydrazine solution in order to cleave the DDE linker or DTT to cleave the DS linker (where appropriate). After nano-LC−MS/MS analysis, raw data were searched using Proteome Discoverer to identify peptides with the corresponding chemical remnant, and corresponding PSMs were validated manually to confirm proper localization based on the presence of site-determining ions.

Interestingly, linker remnants were exclusively found on the side chains of Asp and Glu residues. This is in line with the recent finding that aliphatic diazirines, when irradiated, isomerize to the diazo form to a larger extent than aromatic diazirines, and these preferentially label carboxylic acids.[32] As expected, our in-gel subtilisin digestion yielded high sequence coverages of calmodulin (full-length, >91%) and GPL1-R (amino acids 24−154, >89%), with all Asp and Glu residues of the two proteins being covered. For calmodulin, we identified peptide/protein crosslinks on E12 (ds), E83 (ds), and E85 (ds and dde; Figure 3C). For GLP1-R, we identified D53 (dde) (Figure S1). Notably, all the identified modified spectra were also compared to PSMs of the same peptide sequence without modification, to increase the confidence of identifications. As previously observed for our synthetic peptides, the retention time differences between the nonmodified and dde-modified peptides were small but more pronounced for ds-modified peptides (compare Figure 2A and C).

After the identification of the photoaffinity labeling sites, we mapped these onto crystal structures of the proteins. For the GLP-1R, a cocrystal structure with GLP-1 is available.[37] In this structure, the modification site D53 is located relatively far from the lysine residue and the N-terminus of the glucagon peptide (Figure S2). However, there are several reports on oligomerization[38,39] as well as structural flexibility of the GLP-1R. The latter involves flexibility of the extracellular domain relative to the transmembrane domains[40,41] but also differences in interactions by different peptide agonists.[42] As this complicates interpretation, we therefore further focused on the melittin−calmodulin interaction. Here, we found three modification sites, two of which are located close to each other on the same helix (E83 and E85), whereas the third one (E11) is localized on a different helix (Figure 4A). These sites can be rationalized in two ways. First, melittin has multiple lysine residues as well as a free N-terminus, and each can react with the succinimide reagent **9** or **13**. Therefore, we would expect crosslinking at various sites of the protein target, in line with our findings. Second, previous crosslinking studies have suggested that melittin has two different binding modes to calmodulin,[43] in which the helical melittin binds in a groove of calmodulin in either a C- to N-terminal orientation or vice versa (Figure 4B,C). Hence, the cleavable photoreactive group on one end of the melittin may reach either side of the calmodulin.

CONCLUSIONS

Here, we reported on cleavable photoreactive building blocks for photocrosslinking peptide ligands to protein receptors. Starting with various MS-cleavable and chemically cleavable linkers, we found that DDE and DS cleavable linkers performed best in terms of their LC−MS/MS peptide identification, while they also display mild and convenient chemically cleavable properties. Trifunctional reagents **9** and **13**, which contain a DDE or DS cleavable linker, a diazirine photoreactive group that has a small steric footprint and a succinimide ester for functionalization of free amines, allow conjugation to small peptides and crosslinking them to protein

https://doi.org/10.1021/acsomega.3c03064
ACS Omega 2023, 8, 25487−25495

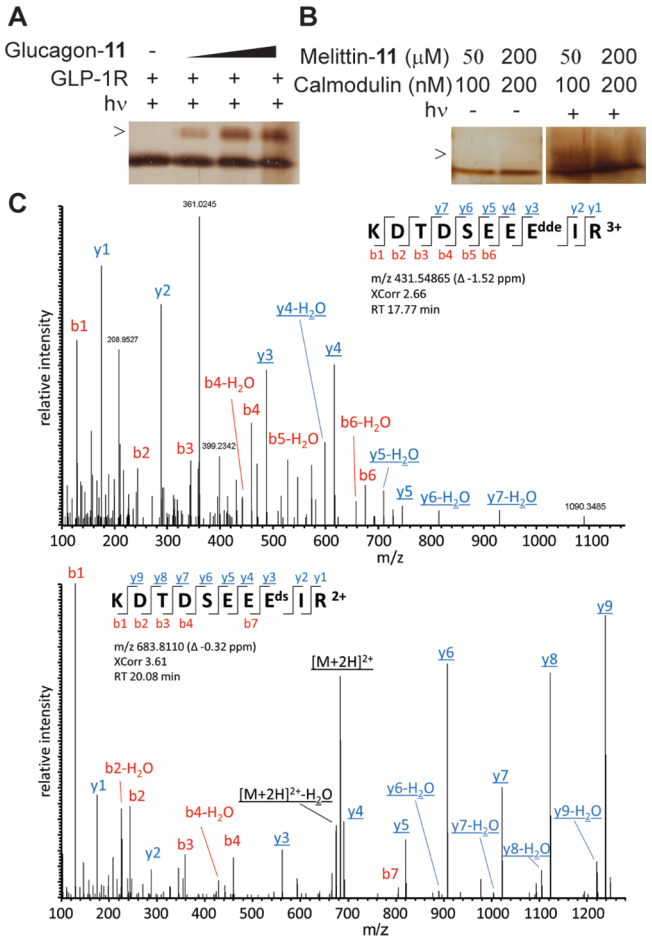

Figure 3. Photoaffinity modification of proteins by peptide ligands equipped with building block **13**. (A) GLP-1R is covalently modified by increasing concentrations of the glucagon−**13** conjugate. (B) Calmodulin is modified by the melittin−**13** conjugate upon UV irradiation (right panel) but not when excluded from light (left panel). (C) Modification of calmodulin at E85 identifies the potential calmodulin/melittin interaction site. Representative MS/MS spectrum of the calmodulin dde-modified peptide KDTDSEEE(*dde*)IR (upper panel) and its ds-modified counterpart (lower panel), obtained after digestion with subtilisin (sequence coverage in ds and dde samples of >92%). Identified b ions (red) and y ions (blue) cover the full peptide sequence, with y2/y3 fragment ions allowing a clear localization of the modification at Glu85 (all fragment ions containing the ds/dde remnant are underlined). All highlighted fragment ions were matched with a maximum deviation of 10 ppm from their theoretical masses. RT = retention time; Δppm = deviation from theoretical mass in ppm; XCorr = Sequest Cross correlation score.

receptors. We demonstrate that after cleavage, modified peptides can be identified by MS/MS by using the small modification remnant as variable modification. As we demonstrate for melittin/calmodulin binding, our strategy allows mapping of peptide/protein interactions. Importantly, we found that two different cleavable linkers (DDE and DS) led to the identification of the same crosslinking site on calmodulin (E85), underlining the reliability of crosslinking and the validity of our approach.

Overall, we expect this strategy to be widely applicable for the study of peptide−protein interactions. Although we here used trifunctional reagents to modify commercial peptides, these building blocks may also be applied in solid-phase peptide synthesis for custom synthesis of modified peptides. In addition to the use on purified proteins, the here described strategy may also be exploited in complex mixtures, provided that the peptides are modified with a purification handle, such as a biotin or an azide/alkyne for biorthogonal modification. This would allow to specifically screen for interaction partners of bioactive polypeptides within whole proteomes. We think that the method described here is particularly relevant, as peptides are gaining increasing attention as drugs and drug candidates owing to their high specificity and relatively straightforward modular synthesis.[46,47] It will therefore help in gaining a better understanding of the interaction between bioactive peptides and their protein targets.

EXPERIMENTAL SECTION

Synthesis. Details on the synthesis of compounds and their characterization are given in the Supporting Information.

Analysis of Synthetic Test Peptides. To assess the suitability of the different linker chemistries, the model missed-cleavage tryptic peptides LFLKSGVR and VKAALELAEQR were selected, and their internal Lys residues were modified with the different MS-cleavable or chemically cleavable linkers. All different peptides were analyzed by LC−MS/MS on three different mass spectrometers (Q Exactive Plus, Orbitrap Fusion, and Triple TOF 6600) with and without prior cleavage. Different fragmentation modes were used: collision-induced dissociation (CID), electron transfer dissociation (ETD), higher-energy collisional dissociation (HCD), and EtHCD (combining ETD with supplemental HCD). The resulting data were searched using Proteome Discoverer 2.4 with two search engines (MS Amanda[48] and Sequest HT[49]), and the efficiency of cleavage was assessed by comparing the peak areas of the noncleaved peptides (DDE, AZ, DS, SF, UA, and UB) between samples with and without cleavage treatment.

Modification of Peptides. Coupling reactions between cleavable linkers (**9** and **13**) and peptides (glucagon and melittin) were performed in DMSO, with a final peptide concentration of 1 mM. Stock solutions of peptides and linkers were at 25 mM in DMSO. Reactions were stirred overnight at room temperature after each addition of the linker and the base. For modification of glucagon, 0.5 equiv of the linker and 0.6 equiv of DIPEA were initially added, and the reaction was monitored by LC−MS to assess conversion to the mono-substituted peptide (unmodified and polysubstituted peptides were also present but generally to a lesser extent, see Figures S3−S6). Additional equivalents of the linker (0.25 equiv) and DIPEA (0.3 equiv) were added as required until the monosubstituted peptide was the dominant species as measured by LC−MS. For modification of melittin, 1 equiv of the linker and 1.2 equiv of DIPEA were initially added, with additional equivalents of the linker (0.5 equiv) and DIPEA (0.6 equiv) added until the monosubstituted peptide was the dominant species as measured by LC−MS.

PAL of Proteins with Modified Peptides. A 25 mM DMSO stock (1.5 μL) of the modified peptide (final concentration of 200 μM) was added to a solution of protein (1.2 μg) in 180 μL of reaction buffer (calmodulin: 50 mM HEPES, 150 mM NaCl, and 0.5% v/v NP-40, pH 7.4, GLP-1R: 0.1 M sodium acetate buffer, pH 4). The reactions were incubated for 1 h at 37 °C, after which they were irradiated for 6 min using a UVPTM Blak-Ray B-100AP high-intensity UV lamp (230 V, 100 W). Subsequently, 720 μL of ice-cold acetone was added, and the reaction mixtures were vortexed

https://doi.org/10.1021/acsomega.3c03064
ACS Omega 2023, 8, 25487−25495

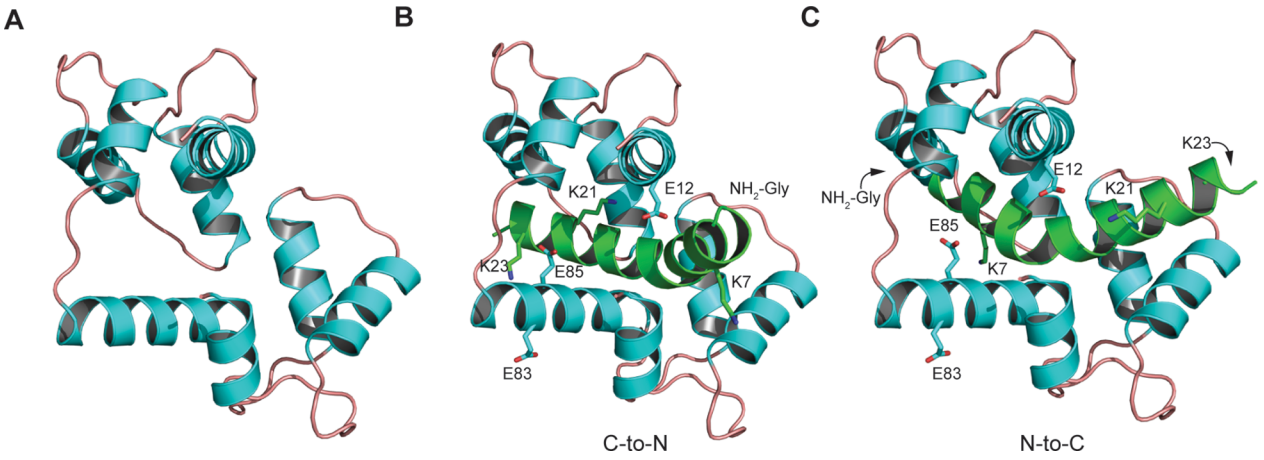

Figure 4. Mapping of binding sites on proteins. (A) Crystal structure of calmodulin (PDB code 1CDL). Helices depicted in cyan and random coils in pink. Picture rendered with PyMol.[44] (B,C) In silico models of the calmodulin−melittin, generated by ZDOCK,[45] show two orientations of binding as suggested by prior experimental crosslinking data.[43] Melittin is depicted in green. The lysine side chains and crosslinked glutamate residues are depicted in a stick model.

briefly before being left at −20 °C for 48 h. The precipitated protein was collected by centrifugation at 5000*g* for 1 min and then at 17,000*g* for 5 min using a benchtop centrifuge. The supernatant was removed, and the pellet was washed once with ice-cold acetone. The pellet was left to air-dry for 5 min and redissolved in 1× sample buffer. Proteins were resolved on a 12% acrylamide gel and visualized by silver stain (Pierce silver stain for mass spectrometry).

LC−MS/MS Analysis of Crosslinked Protein−Peptide Pairs. *In-Gel Digestion.* Gel bands were cut using a scalpel and placed in a tube for protein digestion. Salts and detergents were removed from gel bands by subsequent washing with 50 μL of 50 mM ammonium bicarbonate (ABC) for 10 min at 37 °C followed by 50 μL of 50% acetonitrile (ACN) in 50 mM ABC for 10 min at 37 °C, repeated twice. DDE samples were then incubated in 10 mM dithiothreitol (DTT) and 50 mM ABC for 30 min at 56 °C for reduction, and all samples were alkylated in 5 mM iodoacetamide (IAA) for 30 min in the dark. Gel bands were then washed in 50 μL of 50 mM ABC for 10 min at 37 °C followed by 50 μL of 50% ACN in 50 mM ABC for 10 min at 37 °C, repeated twice. Next, gel bands were dried in a speed vac. Subtilisin digestion was performed analogous to a reported procedure.[36] In short, subtilisin digestion solution was prepared at a concentration of 12.5 ng/μL of the enzyme in 50 mM ABC. The digestion solution (20 μL) was added to each dried gel band and incubated at 4 °C for 10 min. Then, excess solution was removed followed by a 30 min incubation at 56 °C. In order to quench the reaction, 15 μL of 0.1% TFA was added to the gel piece and incubated for 15 min under shaking. The supernatant was transferred to a fresh tube, and another 15 μL of 0.1% TFA was added to the gel piece for another 15 min. Finally, 15 μL of 50% ACN in 0.1% TFA was added to the gel piece, incubated for 15 min, and transferred to the tube. Samples were dried in the speed vac and stored at −40 °C.

Cleavage. DDE linker-modified peptides were resuspended in 4% hydrazine and incubated for 60 min at 40 °C. Disulfide linker-modified peptides were resuspended in 50 mM DTT and incubated for 30 min at room temperature. Control samples (digested proteins not treated with a probe) were treated the same. For desalting, a column was prepared using Empore octadecyl C18 extraction disks (Sigma Aldrich, cat. no. 66883-U) and 10 μL of R3 resin (Thermo Scientific) at 25 μg/μL in 90% ACN. The column was washed three times with 100% ACN and equilibrated with 0.1% TFA three times. Following the washing and equilibration steps, samples were added to the column and centrifuged at 1500*g* for 5 min. The loading step was repeated three times, and samples were washed with 0.1% TFA three times. Finally, peptides were eluted in 70% ACN and 0.1% TFA and dried in a speed vac. Samples were reconstituted in 0.1% formic acid.

Nano-LC−MS/MS. Samples were analyzed by nano-LC−MS/MS on a Q Exactive Plus, coupled to an Easy-nLC 1200 (both Thermo Fisher Scientific). The LC system was equipped with an AcclaimPepMap 100 C18 precolumn (Thermo Fisher Scientific, 3 μm particle size, 75 μm inner diameter × 2 cm length) and a nanoscale analytical column (Thermo Fisher Scientific, AcclaimPepMap 100 C18 main column, 2 μm particle size, 75 μm inner diameter × 25 cm length). Samples were separated using a binary gradient (solvent A: 0.1% formic acid, solvent B: 0.1% formic acid and 84% acetonitrile) ranging from 0 to 40% in 30 min at a flow rate of 300 nL/min. MS scans were acquired from m/z 350 to 1500 at a resolution of 70,000 with an automatic gain control (AGC) of 1e6 and a maximum injection time of 50 ms. The seven most intense parent ions with charge states of +2 to +4 were isolated with a window of m/z 1.2, an AGC of 5e4, and a maximum injection time of 220 ms and fragmented with a normalized collision energy of 28 using a dynamic exclusion of 5 s.

Database Search. MS raw data were searched using Proteome Discoverer 2.4 (Thermo Scientific), using Sequest HT and a human SwissProt FASTA database (20,387 forward sequences, downloaded October 2020). The enzyme was set to either trypsin with a maximum of 1 missed cleavage or to "no enzyme" (subtilisin). Mass tolerances were set to 10 ppm for MS and 0.02 Da for MS/MS scans. Cleaved DDE (71.074 Da) and cleaved DS (+145.056 Da) were allowed as variable modifications on all amino acids. Based on the manual inspection of the obtained peptide-spectrum matches (PSM) indicating the sole modification of Asp and Glu, which is in line with the literature, we later narrowed down the variable modification to Asp and Glu for final searches. Oxidation of Met (+15.995 Da) was another variable modification, and carbamidomethylation of Cys (+57.021) was used as fixed

https://doi.org/10.1021/acsomega.3c03064
ACS Omega 2023, 8, 25487−25495

modification. Because the probability of a spectrum to match the target protein (either GLP1-R or calmodulin) by chance in a background of >20,000 target sequences is lower than typically used peptide false discovery rates of 0.01, all peptide-spectrum matches (PSM) for dde/ds-modified GLP1-R/calmodulin peptides with a mass deviation of <2 ppm and a Sequest XCorr of >2.0 were manually inspected.

■ ASSOCIATED CONTENT

Supporting Information

The Supporting Information is available free of charge at https://pubs.acs.org/doi/10.1021/acsomega.3c03064.

Supporting schemes describing the synthesis; supporting figures with MS spectra, MS/MS spectra, and representation of the GLP1-GLP1 receptor crystal structure; supporting tables with additional information on the synthesized peptides; additional experimental details on the synthetic methodologies (PDF)

■ AUTHOR INFORMATION

Corresponding Authors

René P. Zahédi − *Segal Cancer Proteomics Centre, Lady Davis Institute for Medical Research and McGill University, Montreal, Quebec H3T 1E2, Canada; Manitoba Centre for Proteomics and Systems Biology, Winnipeg, Manitoba R3E 3P4, Canada; Department of Internal Medicine, University of Manitoba, Winnipeg, Manitoba R3E 0Z2, Canada; Department of Biochemistry and Medical Genetics, University of Manitoba, Winnipeg, Manitoba R3E 3N4, Canada; Cancer Care Manitoba Research Institute, Winnipeg, Manitoba R3E 0V9, Canada*; Email: rene.zahedi@umanitoba.ca

Steven H. L. Verhelst − *Laboratory of Chemical Biology, Department of Cellular and Molecular Medicine, KU Leuven−University of Leuven, Leuven 3000, Belgium; AG Chemical Proteomics, Leibniz Institute for Analytical Sciences ISAS, e.V., Dortmund 44227, Germany*; orcid.org/0000-0002-7400-1319; Email: steven.verhelst@kuleuven.be

Authors

Dimitris Korovesis − *Laboratory of Chemical Biology, Department of Cellular and Molecular Medicine, KU Leuven−University of Leuven, Leuven 3000, Belgium;* Present Address: Institute of Molecular Biology and Biotechnology, Foundation for Research and Technology—Hellas, GR-70013 Heraklion, Greece (D.K.)

Vanessa P. Gaspar − *Segal Cancer Proteomics Centre, Lady Davis Institute for Medical Research and McGill University, Montreal, Quebec H3T 1E2, Canada; Gerald Bronfman Department of Oncology, McGill University, Montreal, Quebec H4A 3T2, Canada;* Present Address: Rosalind and Morris Goodman Cancer Institute, McGill University, 1160 Pine Avenue West, Montreal, QC H3A 1A3, Canada (V.P.G.).

Hester A. Beard − *Laboratory of Chemical Biology, Department of Cellular and Molecular Medicine, KU Leuven−University of Leuven, Leuven 3000, Belgium;* Present Address: Illumina, Inc., Illumina Centre, 19 Granta Park, Great Abingdon, Cambridge CB21 6DF, United Kingdom (H.A.B.); orcid.org/0000-0002-7942-410X

Suyuan Chen − *AG Chemical Proteomics, Leibniz Institute for Analytical Sciences ISAS, e.V., Dortmund 44227, Germany*

Complete contact information is available at: https://pubs.acs.org/10.1021/acsomega.3c03064

Author Contributions

[&]D.K., V.P.G., and H.A.B. contributed equally.

Author Contributions

D.K., H.A.B., and S.C. synthesized linkers, D.K. and H.A.B. synthesized peptides and other reagents and performed photoaffinity labeling, V.P.G. performed proteomics experiments, V.P.G. and R.P.Z. performed proteomics data analysis, and R.P.Z. and S.H.L.V. conceived and supervised the project. All authors have given approval to the final version of the manuscript.

Notes

The authors declare no competing financial interest.

■ ACKNOWLEDGMENTS

We acknowledge funding by FWO (Grant G0D7118N), FRQ (Grant G0D7118N), Stichting Alzheimer Onderzoek, the Chinese Scholarship Council (fellowship to S.C.), the Ministerium für Kultur und Wissenschaft des Landes Nordrhein-Westfalen, the Regierende Bürgermeister von Berlin, and the Bundesministerium für Bildung und Forschung. R.P.Z. is grateful for financial support from the University of Manitoba and Shared Health Manitoba.

■ REFERENCES

(1) Almeida, J. R.; Resende, L. M.; Watanabe, R. K.; Carregari, V. C.; Huancahuire-Vega, S.; Caldeira, C. A. D. A.; Coutinho-Neto, A.; Soares, A. M.; Vale, N.; Gomes, P. A. D. C.; Marangoni, S.; Calderon, L. D. A.; Da Silva, S. L. Snake Venom Peptides and Low Mass Proteins: Molecular Tools and Therapeutic Agents. *Curr. Med. Chem.* **2017**, *24*, 3254.

(2) Nongonierma, A. B.; FitzGerald, R. J. The Scientific Evidence for the Role of Milk Protein-Derived Bioactive Peptides in Humans: A Review. *J. Funct. Foods.* **2015**, 640−656.

(3) Kalra, S.; Sahay, R. A Review on Semaglutide: An Oral Glucagon-Like Peptide 1 Receptor Agonist in Management of Type 2 Diabetes Mellitus. *Diabetes Ther.* **2020**, *2020*, 1965.

(4) Mookherjee, N.; Anderson, M. A.; Haagsman, H. P.; Davidson, D. J. Antimicrobial Host Defence Peptides: Functions and Clinical Potential. *Nat. Rev. Drug Disc.* **2020**, 311−332.

(5) Saghatelian, A.; Couso, J. P. Discovery and Characterization of SmORF-Encoded Bioactive Polypeptides. *Nat. Chem. Biol.* **2015**, 909−916.

(6) Lomenick, B.; Hao, R.; Jonai, N.; Chin, R. M.; Aghajan, M.; Warburton, S.; Wang, J.; Wu, R. P.; Gomez, F.; Loo, J. A.; Wohlschlegel, J. A.; Vondriska, T. M.; Pelletier, J.; Herschman, H. R.; Clardy, J.; Clarke, C. F.; Huang, J. Target Identification Using Drug Affinity Responsive Target Stability (DARTS). *Proc. Natl. Acad. Sci. U. S. A.* **2009**, *106*, 21984−21989.

(7) Piazza, I.; Kochanowski, K.; Cappelletti, V.; Fuhrer, T.; Noor, E.; Sauer, U.; Picotti, P. A Map of Protein-Metabolite Interactions Reveals Principles of Chemical Communication. *Cell* **2018**, *172*, 358−372.e23.

(8) Savitski, M. M.; Reinhard, F. B.; Franken, H.; Werner, T.; Savitski, M. F.; Eberhard, D.; Martinez Molina, D.; Jafari, R.; Dovega, R. B.; Klaeger, S.; Kuster, B.; Nordlund, P.; Bantscheff, M.; Drewes, G. Tracking Cancer Drugs in Living Cells by Thermal Profiling of the Proteome. *Science* **2014**, *346*, 1255784.

(9) Iacobucci, C.; Götze, M.; Sinz, A. Cross-Linking/Mass Spectrometry to Get a Closer View on Protein Interaction Networks. *Curr. Opin. Biotechnol.* **2020**, 48−53.

(10) Steigenberger, B.; Albanese, P.; Heck, A. J. R.; Scheltema, R. A. To Cleave or Not to Cleave in XL-MS? *J. Am. Soc. Mass Spectrom.* **2020**, *31*, 196−206.
(11) Belsom, A.; Rappsilber, J. Anatomy of a Crosslinker. *Curr. Opin.Chem. Biol.* **2021**, 39−46.
(12) Tang, X.; Wippel, H. H.; Chavez, J. D.; Bruce, J. E. Crosslinking Mass Spectrometry: A Link between Structural Biology and Systems Biology. *Protein Sci.* **2021**, 773−784.
(13) Petrotchenko, E. V.; Borchers, C. H. Crosslinking Combined with Mass Spectrometry for Structural Proteomics. *Mass Spectrom. Rev.* **2010**, *29*, 862−876.
(14) Sinz, A. Divide and Conquer: Cleavable Cross-Linkers to Study Protein Conformation and Protein − Protein Interactions. *Anal. Bioanal. Chem.* **2017**, *409*, 33−44.
(15) Plaschka, C.; Larivière, L.; Wenzeck, L.; Seizl, M.; Hemann, M.; Tegunov, D.; Petrotchenko, E. V.; Borchers, C. H.; Baumeister, W.; Herzog, F.; Villa, E.; Cramer, P. Architecture of the RNA Polymerase II-Mediator Core Initiation Complex. *Nature* **2015**, *518*, 376−380.
(16) Linden, A.; Deckers, M.; Parfentev, I.; Pflanz, R.; Homberg, B.; Neumann, P.; Ficner, R.; Rehling, P.; Urlaub, H. A Cross-Linking Mass Spectrometry Approach Defines Protein Interactions in Yeast Mitochondria. *Mol. Cell. Proteomics* **2020**, *19*, 1161−1178.
(17) Makepeace, K. A. T.; Mohammed, Y.; Rudashevskaya, E. L.; Petrotchenko, E. V.; Vögtle, F.-N.; Meisinger, C.; Sickmann, A.; Borchers, C. H. Improving Identification of In-Organello Protein-Protein Interactions Using an Affinity-Enrichable, Isotopically-Coded, and Mass Spectrometry-Cleavable Chemical Crosslinker. *Mol. Cell. Proteomics* **2020**, *19*, 624−639.
(18) Gomkale, R.; Linden, A.; Neumann, P.; Schendzielorz, A. B.; Stoldt, S.; Dybkov, O.; Kilisch, M.; Schulz, C.; Cruz-Zaragoza, L. D.; Schwappach, B.; Ficner, R.; Jakobs, S.; Urlaub, H.; Rehling, P. Mapping Protein Interactions in the Active TOM-TIM23 Supercomplex. *Nat. Commun.* **2021**, *12*, 5715.
(19) Dubinsky, L.; Krom, B. P.; Meijler, M. M. Diazirine Based Photoaffinity Labeling. *Bioorg. Med. Chem.* **2012**, *20*, 554−570.
(20) Geurink, P. P.; Prely, L. M.; van der Marel, G. A.; Bischoff, R.; Overkleeft, H. S. Photoaffinity Labeling in Activity-Based Protein Profiling. *Top. Curr. Chem.* **2011**, *324*, 85−113.
(21) Smith, E.; Collins, I. Photoaffinity Labeling in Target- and Binding-Site Identification. *Future Med. Chem.* **2015**, *7*, 159−183.
(22) Burton, N. R.; Kim, P.; Backus, K. M. Photoaffinity Labelling Strategies for Mapping the Small Molecule-Protein Interactome. *Org. Biomol. Chem.* **2021**, 7792−7809.
(23) Parker, B. W.; Goncz, E. J.; Krist, D. T.; Statsyuk, A. V.; Nesvizhskii, A. I.; Weiss, E. L. Mapping Low-Affinity/High-Specificity Peptide−Protein Interactions Using Ligand-Footprinting Mass Spectrometry. *Proc. Natl. Acad. Sci. U. S. A.* **2019**, *116*, 21001−21011.
(24) Nguyen, M. T. N.; Shema, G.; Zahedi, R. P.; Verhelst, S. H. L. Protease Specificity Profiling in a Pipet Tip Using "Charge-Synchronized" Proteome-Derived Peptide Libraries. *J. Proteome Res.* **2018**, *17*, 1923−1933.
(25) Kao, A.; Chiu, C. L.; Vellucci, D.; Yang, Y.; Patel, V. R.; Guan, S.; Randall, A.; Baldi, P.; Rychnovsky, S. D.; Huang, L. Development of a Novel Cross-Linking Strategy for Fast and Accurate Identification of Cross-Linked Peptides of Protein Complexes. *Mol. Cell. Proteomics* **2011**, *10*, No. 002212.
(26) Müller, M. Q.; Dreiocker, F.; Ihling, C. H.; Schäfer, M.; Sinz, A. Cleavable Cross-Linker for Protein Structure Analysis: Reliable Identification of Cross-Linking Products by Tandem MS. *Anal. Chem.* **2010**, *82*, 6958−6968.
(27) Verhelst, S. H. L.; Fonovic, M.; Bogyo, M. A Mild Chemically Cleavable Linker System for Functional Proteomic Applications. *Angew. Chem., Int. Ed.* **2007**, *46*, 1284−1286.
(28) Fonovic, M.; Verhelst, S. H. L.; Sorum, M. T.; Bogyo, M. Proteomics Evaluation of Chemically Cleavable Activity-Based Probes. *Mol. Cell. Proteomics* **2007**, *6*, 1761−1770.
(29) Wu, S. L.; Jiang, H.; Lu, Q.; Dai, S.; Hancock, W. S.; Karger, B. L. Mass Spectrometric Determination of Disulfide Linkages in Recombinant Therapeutic Proteins Using Online LC-MS with Electron-Transfer Dissociation. *Anal. Chem.* **2009**, *81*, 112−122.
(30) Yang, Y.; Verhelst, S. H. L. Cleavable Trifunctional Biotin Reagents for Protein Labelling, Capture and Release. *Chem. Commun.* **2013**, *49*, 5366−5368.
(31) Mnatsakanyan, R.; Markoutsa, S.; Walbrunn, K.; Roos, A.; Verhelst, S. H. L.; Zahedi, R. P. Proteome-Wide Detection of S-Nitrosylation Targets and Motifs Using Bioorthogonal Cleavable-Linker-Based Enrichment and Switch Technique. *Nat. Commun.* **2019**, *10*, 2195.
(32) West, A. V.; Muncipinto, G.; Wu, H.-Y.; Huang, A. C.; Labenski, M. T.; Jones, L. H.; Woo, C. M. Labeling Preferences of Diazirines with Protein Biomolecules. *J. Am. Chem. Soc.* **2021**, *143*, 6691−6700.
(33) Kleiner, P.; Heydenreuter, W.; Stahl, M.; Korotkov, V. S.; Sieber, S. A. A Whole Proteome Inventory of Background Photocrosslinker Binding. *Angew. Chem., Int. Ed.* **2017**, *56*, 1396−1401.
(34) Berman, H. M.; Westbrook, J.; Feng, Z.; Gilliland, G.; Bhat, T. N.; Weissig, H.; Shindyalov, I. N.; Bourne, P. E. The Protein Data Bank. *Nucleic Acids Res.* **2000**, 235−242.
(35) Gonczarowska-Jorge, H.; Dell'Aica, M.; Dickhut, C.; Zahedi, R. P. Variable Digestion Strategies for Phosphoproteomics Analysis. *Methods Mol. Biol.* **2016**, *1355*, 225−239.
(36) Gonczarowska-Jorge, H.; Loroch, S.; Dell'Aica, M.; Sickmann, A.; Roos, A.; Zahedi, R. P. Quantifying Missing (Phospho)Proteome Regions with the Broad-Specificity Protease Subtilisin. *Anal. Chem.* **2017**, *89*, 13137−13145.
(37) Underwood, C. R.; Garibay, P.; Knudsen, L. B.; Hastrup, S.; Peters, G. H.; Rudolph, R.; Reedtz-Runge, S. Crystal Structure of Glucagon-like Peptide-1 in Complex with the Extracellular Domain of the Glucagon-like Peptide-1 Receptor. *J. Biol. Chem.* **2010**, *285*, 723−730.
(38) Song, X.; Yu, Y.; Shen, C.; Wang, Y.; Wang, N. Dimerization/Oligomerization of the Extracellular Domain of the GLP-1 Receptor and the Negative Cooperativity in Its Ligand Binding Revealed by the Improved NanoBiT. *FASEB J.* **2020**, *34*, 4348−4368.
(39) Koole, C.; Reynolds, C. A.; Mobarec, J. C.; Hick, C.; Sexton, P. M.; Sakmar, T. P. Genetically Encoded Photocross-Linkers Determine the Biological Binding Site of Exendin-4 Peptide in the N-Terminal Domain of the Intact Human Glucagon-like Peptide-1 Receptor (GLP-1R). *J. Biol. Chem.* **2017**, *292*, 7131−7144.
(40) Yang, D.; De Graaf, C.; Yang, L.; Song, G.; Dai, A.; Cai, X.; Feng, Y.; Reedtz-Runge, S.; Hanson, M. A.; Yang, H.; Jiang, H.; Stevens, R. C.; Wang, M. W. Structural Determinants of Binding the Seventransmembrane Domain of the Glucagon-like Peptide-1 Receptor (GLP-1R). *J. Biol. Chem.* **2016**, *291*, 12991−13004.
(41) Wu, F.; Yang, L.; Hang, K.; Laursen, M.; Wu, L.; Han, G. W.; Ren, Q.; Roed, N. K.; Lin, G.; Hanson, M. A.; Jiang, H.; Wang, M. W.; Reedtz-Runge, S.; Song, G.; Stevens, R. C. Full-Length Human GLP-1 Receptor Structure without Orthosteric Ligands. *Nat. Commun.* **2020**, *11*, 1272.
(42) Deganutti, G.; Liang, Y. L.; Zhang, X.; Khoshouei, M.; Clydesdale, L.; Belousoff, M. J.; Venugopal, H.; Truong, T. T.; Glukhova, A.; Keller, A. N.; Gregory, K. J.; Leach, K.; Christopoulos, A.; Danev, R.; Reynolds, C. A.; Zhao, P.; Sexton, P. M.; Wootten, D. Dynamics of GLP-1R Peptide Agonist Engagement Are Correlated with Kinetics of G Protein Activation. *Nat. Commun.* **2022**, *13*, 92.
(43) Schulz, D. M.; Ihling, C.; Clore, G. M.; Sinz, A. Mapping the Topology and Determination of a Low-Resolution Three-Dimensional Structure of the Calmodulin-Melittin Complex by Chemical Cross-Linking and High-Resolution FTICRMS: Direct Demonstration of Multiple Binding Modes. *Biochemistry* **2004**, *43*, 4703−4715.
(44) Delano, W. L. *The Pymol Molecular Graphics Systems* (Http://Www.Pymol.Org). 2002.
(45) Pierce, B. G.; Wiehe, K.; Hwang, H.; Kim, B. H.; Vreven, T.; Weng, Z. ZDOCK Server: Interactive Docking Prediction of Protein-Protein Complexes and Symmetric Multimers. *Bioinformatics* **2014**, *30*, 1771−1773.

https://doi.org/10.1021/acsomega.3c03064
ACS Omega 2023, 8, 25487−25495

(46) Angell, Y.; Holford, M.; Moos, W. H. Building on Success: A Bright Future for Peptide Therapeutics. *Protein Pept. Lett.* **2019**, *25*, 1044−1050.
(47) Henninot, A.; Collins, J. C.; Nuss, J. M. The Current State of Peptide Drug Discovery: Back to the Future? *J. Med. Chem.* **2018**, 1382−1414.
(48) Dorfer, V.; Strobl, M.; Winkler, S.; Mechtler, K. MS Amanda 2.0: Advancements in the Standalone Implementation. *Rapid Commun. Mass Spectrom.* **2021**, *35*, No. e9088.
(49) Eng, J. K.; McCormack, A. L.; Yates, J. R. An Approach to Correlate Tandem Mass Spectral Data of Peptides with Amino Acid Sequences in a Protein Database. *J. Am. Soc. Mass Spectrom.* **1994**, *5*, 976−989.

https://doi.org/10.1021/acsomega.3c03064
ACS Omega 2023, 8, 25487−25495